HHS Public Access

Author manuscript

J Neurol Sci. Author manuscript; available in PMC 2024 November 15.

Published in final edited form as:

J Neurol Sci. 2023 November 15; 454: 120828. doi:10.1016/j.jns.2023.120828.

Lysine 117 on ataxin-3 modulates toxicity in *Drosophila* models of Spinocerebellar Ataxia Type 3

Jessica R. Blount[1,*], **Nikhil C. Patel**[1,*], **Kozeta Libohova**[1], **Autumn L. Harris**[1,2], **Wei-Ling Tsou**[1], **Alyson Sujkowski**[1,#], **Sokol V. Todi**[1,2,3,#]

[1]-Department of Pharmacology, Wayne State University

[2]-Maximizing Access to Research Careers, Wayne State University

[3]-Department of Neurology, Wayne State University

Abstract

Ataxin-3 (Atxn3) is a deubiquitinase with a polyglutamine (polyQ) repeat tract whose abnormal expansion causes the neurodegenerative disease, Spinocerebellar Ataxia Type 3 (SCA3; also known as Machado-Joseph Disease). The ubiquitin chain cleavage properties of Atxn3 are enhanced when the enzyme is itself ubiquitinated at lysine (K) at position 117: in vitro, K117-ubiqutinated Atxn3 cleaves poly-ubiquitin markedly more rapidly compared to its unmodified counterpart. How polyQ expansion causes SCA3 remains unclear. To gather insights into the biology of disease of SCA3, here we posited the question: is K117 important for toxicity caused by pathogenic Atxn3? To answer this question, we generated transgenic *Drosophila* lines that express full-length, human, pathogenic Atxn3 with 80 polyQ with an intact or mutated K117. We found that mutating K117 mildly enhances the toxicity and aggregation of pathogenic Atxn3. An additional transgenic line that expresses Atxn3 without any K residues confirms increased aggregation of pathogenic Atxn3 whose ubiquitination is perturbed. These findings suggest that Atxn3 ubiquitination is a regulatory step of SCA3, in part by modulating its aggregation.

[#]:Correspondence: asujkows@med.wayne.edu; stodi@wayne.edu.

[*]These authors contributed equally to this manuscript

AUTHOR CONTRIBUTIONS:

JRB: conceptualization, data curation, software, formal analysis, validation, investigation, visualization, methodology, and editing.

NCP: data curation, software, formal analysis, validation, investigation, visualization, methodology, and editing.

KL: data curation, validation, investigation, methodology.

ALH: data curation, funding acquisition, validation, investigation, methodology.

W-LT: conceptualization, data curation, software, formal analysis, validation, investigation, visualization, methodology.

AS: conceptualization, data curation, software, formal analysis, validation, investigation, visualization, methodology, and writing and editing.

SVT: conceptualization, data curation, funding acquisition, software, formal analysis, validation, investigation, visualization, methodology, and writing and editing.

CONFLICT OF INTEREST STATEMENT: The authors declare that they do not have any conflicts of interest to disclose.

INTRODUCTION

The most common, dominantly inherited ataxia worldwide, Spinocerebellar Ataxia Type 3 (SCA3), also known as Machado-Joseph Disease, is caused by a mutation in the deubiquitinase (DUB) ataxin-3 (Atxn3). Atxn3 contains a polyglutamine (polyQ) repeat whose abnormal expansion is pathogenic (Kawaguchi et al., 1994; Stevanin et al., 1995a; Stevanin et al., 1995b). Eight additional proteins have a similar repeat whose lengthening causes neurodegeneration in what is known as the polyQ family of diseases (Johnson et al., 2022b; Paulson et al., 2017; Zoghbi and Orr, 2009).

It is unclear how polyQ expansion in Atxn3 causes SCA3. According to data from animal and cell models of SCA3, polyQ expansion may modify normal functions of Atxn3 as well as endow it with new properties (Dantuma and Herzog, 2020; Johnson et al., 2019; Johnson et al., 2021; Johnson et al., 2022a; Johnson et al., 2020; Matos et al., 2019a). Still, precise molecular sequelae remain uncertain and would benefit from systematic investigations of the disease protein, its partners, and its functions. Towards this end, we have explored the role of ubiquitin (its substrate) on Atxn3. We have found that: wild-type and pathogenic Atxn3 are prominently ubiquitinated in vitro, in cultured cells, in *Drosophila*, and in mouse brain; wild-type and pathogenic Atxn3 are primarily ubiquitinated at lysine (K) at position 117, which resides on the catalytic domain (figure 1A); the catalytic activity of wild-type and pathogenic Atxn3 is markedly enhanced by its own ubiquitination in vitro; neither wild-type nor pathogenic Atxn3 require their own ubiquitination to be degraded by the proteasome (Blount et al., 2020; Blount et al., 2014; Faggiano et al., 2013; Faggiano et al., 2015; Todi et al., 2010; Todi et al., 2009; Tsou et al., 2013; Winborn et al., 2008). These prior results led us to ask: is ubiquitination of Atxn3 important for its toxicity? We reasoned that this question would bear special importance to further understand the pathogenic properties of the SCA3 protein, providing additional pieces to the larger puzzle of the SCA3 biology of disease.

Here, we report the generation and examination of additional *Drosophila* models of SCA3. These transgenic lines express full-length, human Atxn3 with an expanded polyQ repeat with intact or mutated K117, or absent any lysine residues. The lines are isogenic among each other and other pathogenic Atxn3 lines that we reported recently (Johnson et al., 2019; Johnson et al., 2021; Johnson et al., 2022a; Johnson et al., 2020; Prifti et al., 2022); they employ PhiC-31-mediated insertion (Fish et al., 2007; Groth et al., 2004) of the human Atxn3 cDNA into the same genomic locus, in our case site attP2 on chromosome 3 of *Drosophila*. This methodology (Markstein et al., 2008; Ni et al., 2008) ensures that a single copy of the transgene is inserted, in the same orientation, into the same site, enabling similar expression among different transgenic lines and allowing for direct comparison among different Atxn3 mutants. We used the Gal4-UAS binary system of transgene expression in *Drosophila* (Brand et al., 1994; Brand and Perrimon, 1993) to express the UAS-Atxn3 transgenes in various tissues, including throughout the fly, only in fly neurons, or only in fly eyes, and examined flies in terms of longevity and morphology, as well as through biochemical assays. We found that K117 mutation enhances the toxicity of pathogenic Atxn3 in the fruit fly, and that this observation coincides with mildly increased

aggregation of the offending protein. Overall, our studies point to a modest modifier role for ubiquitination of Atxn3 in its toxicity.

RESULTS

Mutation of K117 enhances toxicity of pathogenic Atxn3 in *Drosophila*

To examine the role of K117 in the toxicity of pathogenic Atxn3 (figure 1A), we generated *Drosophila melanogaster* transgenic lines that express one of the following versions of the SCA3 protein: UAS-Atxn3 with 80Q (within human disease range, without any additional mutations (Johnson et al., 2022b)); UAS-Atxn3 with 80Q where K117 is mutated into the similar, but non-ubiquitinatable amino acid arginine (K117R); and a version with 80Q where each of the lysine residues is mutated into an arginine (UAS-Atxn3 KNull; figure 1A). The transgenes consist of the full-length, human cDNA. Each transgene is C-terminally tagged with an HA epitope tag. We previously reported that human Atxn3 with a normal polyQ repeat is not toxic in flies and that mutating lysine residues of an otherwise wild-type Atxn3 does not render it toxic in fly tissues (Blount et al., 2014; Johnson et al., 2020; Prifti et al., 2022; Sutton et al., 2017; Tsou et al., 2013; Tsou et al., 2015b). Therefore, here we focused exclusively on pathogenic Atxn3.

The KNull line was generated to investigate more generally the role of ubiquitination on toxicity from pathogenic Atxn3. There were two reasons for this decision: 1) We had previously reported that although K117 is the primary site of ubiquitination of Atxn3 in vitro and in mammalian cells, other lysines on Atxn3 can also be modified (Todi et al., 2010); 2) Additionally, we had observed that ubiquitination of pathogenic Atxn3 is not required for its degradation in mammalian cell culture (Blount et al., 2020). For the purposes of scientific rigor, we sought to confirm in vivo whether ubiquitination of pathogenic Atxn3 is generally required for its degradation, and whether it plays a role on its toxicity.

We started by examining the toxicity of each UAS-Atxn3 transgene when expressed in all tissues, at all stages. When driven constitutively by sqh-Gal4, we noticed that expression of both Atxn3(Q80) and K117R led to lethality during fly development as pupae and pharate adults (figure 1B). Statistically, K117R led to a higher percentage of developing flies dying as pupae rather than pharate adults, compared to Atxn3(Q80); $p<0.01$. In neither case did we observe any adult flies eclose successfully from their pupal cases (figure 1B). KNull expression, however, significantly improved developmental lethality. Most KNull flies emerged as adults and survived for ~30 days, but their longevity was shorter than the longevity of flies not expressing pathogenic Atxn3 (figure 1C; $p<0.001$). We conclude that lysine mutations impact the toxicity of pathogenic Atxn3 when expressed in all tissues in the fly.

Next, we turned our attention to the toxicity of pathogenic Atxn3 in neurons, the tissue most impacted in SCA3. We expressed each version of pathogenic Atxn3 in all neurons throughout the fly life, or only in adults (figure 2). As shown in figure 2A, constitutive neuronal expression led to differential toxicity: Atxn3(Q80) was more toxic than KNull, but less so than K117R in both males and females. Similarly, expression of these transgenes only in adult fly neurons led to similar differences in toxicity. We did not observe differences

in eclosion among the different genotypes. These results indicate that mutation of K117 enhances the neuronal toxicity of pathogenic Atxn3, whereas mutation of all lysine residues reduces it.

Lysine mutations do not impact the turnover or sub-cellular distribution of pathogenic Atxn3 in flies

Subsequently, we examined biochemical properties of the UAS-Atxn3 versions expressed above. Constitutive, pan-neuronal expression of Atxn3(Q80), K117R and KNull led to similar overall protein levels for Atxn3(Q80) and K117R, but markedly lower levels for KNull (figure 3A; $p<0.01$). According to qRT-PCR, the mRNA levels of Atxn3(Q80) were higher than those of K117R and KNull ($p<0.05$), the latter two being comparable (figure 3B).

We previously observed that lysine-to-arginine codon mutations impact the mRNA levels of wild-type Atxn3 expressed in cultured mammalian cells in the opposite direction of what we noticed here: Atxn3(Q12) mRNA levels were higher when nucleotide mutations substituted all lysines for arginines (Blount et al., 2020). This difference in findings may be due to differential handling of Atxn3 mRNA in cell culture versus in vivo, and could be further due to differences in mRNA because of CAG repeats, 80 (pathogenic) in this case and 12 (normal) in the prior study.

The data in panels 3A and 3B suggest that KNull protein levels are lower than Atxn3(Q80) due to its comparatively low mRNA levels. However, K117R protein levels are similar to Atxn3(Q80), even though the former's mRNA levels are also lower than those of Atxn3(Q80). We thus posited whether the markedly lower levels of KNull Atxn3 stem from higher protein turnover rates. To examine this possibility, we utilized the GeneSwitch system of expression in *Drosophila* (Roman and Davis, 2002). Through this system, the Gal4 driver is inactive until the inducer, RU486, is available. Flies were reared in media without RU486. After they eclosed as adults from their pupal cases, they were placed on media containing RU486 to enable transgene expression for 7 days, which based on our prior work is sufficient to induce abundant UAS transgene expression (Blount et al., 2018). After 7 days, flies were placed on media without RU486, which disallows the expression of any additional Atxn3 while what is already present degrades. As summarized in figure 3C, the rate of dissipation of the three versions of Atxn3 protein is similar, regardless of which lysine residues are present. We interpret these data to indicate that overall ubiquitination of Atxn3 – or only at K117 – is not necessary for its turnover; we have reported this before in mammalian cells and with non-pathogenic Atxn3 in *Drosophila* (Blount et al., 2020; Blount et al., 2014; Todi et al., 2010). According to these results, differences in toxicity between Atxn3(Q80) and K117R are unlikely to be due to difference in the overall protein levels. Reduced toxicity from KNull likely reflects the overall lower protein levels of this construct. We presume that the lower levels of KNull are due to a combination of reduced mRNA levels and translation-dependent degradation. The fact that differences in the mRNA levels between Atxn3(Q80) and K117R do not translate into differences at the overall protein level may be due to variation in the rates of translation versus mRNA stability between these two

constructs; we did not pursue these possibilities further in this work. Overall, we conclude that the turnover of pathogenic Atxn3 protein does not require ubiquitination in vivo.

Because nuclear localization of pathogenic Atxn3 is particularly problematic in mouse models of SCA3 (Bichelmeier et al., 2007; Schmidt et al., 1998), we examined the sub-cellular fractionation of Atxn3 biochemically. We observed a mild trend of increased nucellar presence when K117 ($p=0.53$) or all lysines are mutated ($p=0.16$), compared to Atxn3(Q80), but this did not reach statistical significance. These results suggest that differences in toxicity between Atxn3(Q80) and K117R are unlikely to stem from differences in sub-cellular localization.

DnaJ-1 suppresses the toxicity of pathogenic Atxn3 independently of K117

We and others reported that exogenous expression of various folding-related proteins has marked impact on the toxicity of pathogenic Atxn3 in *Drosophila* and other models of SCA3 (Johnson et al., 2021; Johnson et al., 2020; Joshi et al., 2021; Kakkar et al., 2012; Kazemi-Esfarjani and Benzer, 2000; Kuhlbrodt et al., 2011; Ristic et al., 2018; Tsou et al., 2015a; Tsou et al., 2015b). We wondered whether the protective effect of one such protein, DnaJ-1, which interacts with Atxn3 and is regulated by it (Johnson et al., 2020; Kakkar et al., 2012; Prifti et al., 2022; Tsou et al., 2015b), depends on lysine residues of the SCA3 protein. We expressed either version of pathogenic Atxn3 in adult fly neurons in the absence or presence of exogenous, fruit fly DnaJ-1 (Methods). We found that in each case, exogenous DnaJ-1 improved fly longevity independently of lysine mutations (figure 4A; figure 4B tabulates p values). The median survival index in males is higher than in females in the presence of exogenous DnaJ-1, suggesting sex-dependent effects that are outside the scope of this study, but may require future work.

A note when comparing the results from this figure to those in figure 2B: longevity outcomes from adult neuronal expression in figure 2B are shorter than those in figure 4A. We believe these differences to be due to varying environmental conditions in the lab as these experiments were conducted about 1.5 years apart and may be further accentuated by different batches of fly media components. Still, the overall conclusions about longevity differences show similar trends in both sets of experiments, particularly in females.

Co-immunopurifications (co-IPs) from the same flies did not reveal significant differences in the ability of Atxn3(Q80), K117R ($p=0.44$ compared to (Atxn3Q80)), or KNull ($p=0.22$ compared to (Atxn3Q80)) to interact with DnaJ-1 (figure 4C). Lastly, mRNA levels of DnaJ-1 were not significantly impacted by the various forms of Atxn3 expressed in this study (figure 4D; p values were all 0.99). Due to lack of reliable antibodies to detect endogenous DnaJ-1 protein in the fly, we were not able to examine this co-chaperone at the protein level. We conclude that exogenous DnaJ-1 suppresses the toxicity of pathogenic Atxn3 independently of lysine mutations.

K117 mutation increases mildly the aggregation of pathogenic Atxn3

Thus far, we have observed mild but significant differences in the toxicity Atxn3(Q80) versus K117R; yet, we have not identified clues that elucidate a mechanism underlying these observations: overall protein levels are the same; their turnover is comparable; they

are distributed similarly between cytoplasm and nucleus; and exogenous DnaJ-1 protects successfully against all versions. We next turned our attention to the aggregation of Atxn3 in fly neurons by using biochemistry. In prior work, we found that biochemical aggregation of pathogenic Atxn3 as SDS-resistant species correlates with toxicity, whether measured by changes in longevity, motility, or tissue structure (Johnson et al., 2021; Johnson et al., 2020; Prifti et al., 2022; Ristic et al., 2018; Sutton et al., 2017; Tsou et al., 2015b).

We expressed UAS-Atxn3(Q80), UAS-K117R, or UAS-KNull in adult fly neurons for 1, 7 or 14 days. We then resolved the expressed protein through SDS-PAGE gels and quantified SDS-soluble versus SDS-resistant species for each lane. This protocol focuses on Atxn3 species that remain in the soluble portion of the homogenate (Methods) and includes monomeric and oligomeric species, but not higher-order ones that precipitate because of centrifugation. As summarized in figure 5, we noticed a modestly higher preponderance of SDS-resistant species with K117R compared to Atxn3(Q80) as time progressed, especially in female flies ($p<0.0001$ on days 7 and 14); male flies showed a trend in day 7 ($p=0.09$) and day 14 ($p=0.09$), but did not reach significance. For these comparisons, we quantified the amount of SDS-soluble and SDS-resistant protein in each lane and graphed the soluble portion as a fraction of the total amount of Atxn3 signal in the respective lane. Based on this assay, on days 7 and 14 KNull was consistently more aggregation-prone than either of the other two versions of pathogenic Atxn3, even though the total protein levels of KNull were lower than those of Atxn3(Q80) and K117R, as also shown in figure 3. That is, although the overall levels of KNull Atxn3 are lower than those of the other versions, a higher preponderance of the KNull protein is found in the SDS-resistant smear when compared to its own SDS-soluble levels.

We additionally examined the aggregative propensity of Atxn3(Q80), K117R and KNull by subjecting homogenates from flies with genotypes identical to the ones in figure 5 to a centrifugation protocol that separates proteins into pellet and soluble fractions (supplemental figure 1 and associated protocol), both of which are loaded onto SDS-PAGE gels. Through this technique we can capture monomeric and oligomeric species, as well as higher-order aggregates that would otherwise precipitate during centrifugation with the protocol used in figure 5. This method also suggested increased aggregation of Atxn3 with mutated lysines in adult fly neurons, although the timeline of differences was not the same as in figure 5, likely highlighting the different types of aggregates that the SCA3 protein generates and the ability of each method to identify them. These data from adult neurons suggest a mild trend of increased aggregation of Atxn3(Q80) when K117 or all of its lysines are mutated into arginine residues (figure 5 and supplemental figure 1).

To enhance the overall rigor of our work and to ensure its applicability in other tissues in the fly, we additionally tested the toxicity of pathogenic Atxn3 versions in fly eyes. For the next set of experiments, we used female flies since our findings thus far have applied to both sexes, albeit with some differences in precise timelines and extent of impact. Using a scoring system that we reported in the past (Johnson et al., 2020; Prifti et al., 2022) (figure 6A), we noted that differences among Atxn3(Q80), K117R and KNull that we observed in other tissues are recapitulated in fly eyes: K117 mutation worsens the phenotype observed with Atxn3(Q80), whereas KNull mutations improve them. These differences are

statistically significant on day 21 for Atxn3(Q80) versus Atxn3(Q80)-K117R ($p<0.0001$), and are significant between Atxn3(Q80) and Atxn3(Q80)-KNull at most points examined. At the biochemical level, we observed increased SDS-resistant species with Atxn3(Q80)-K117R and KNull on day 1 compared with Atxn3(Q80) ($p<0.001$), but not at later time points. These collective results suggest that mutating either K117 or all lysine residues on pathogenic Atxn3 can increase its tendency to aggregate in fly tissues.

DISCUSSION

Atxn3, whose polyQ tract expansion causes SCA3, is a DUB. Its enzymatic activity is enhanced by ubiquitination of K117. Here, we asked: is K117 important for the toxicity of pathogenic Atxn3? We found that the answer is yes, but to a mild extent. This answer rests on our fly-based data that expression of pathogenic Atxn3 with a mutated K117 was more toxic than polyQ-expanded Atxn3 with an intact K117 when expressed in various fly tissues and at different stages of the fly life cycle. This mildly enhanced toxicity did not coincide with clear differences in Atxn3 protein levels, its sub-cellular distribution, or its interaction with the co-chaperone DnaJ-1, but correlated with a minor trend of increased aggregation of K117R. Our results do not point to a mechanistic understanding of how the K117R mutation enhances toxicity but provide clues that can be pursued in the future as our understanding of the biology of Atxn3 becomes clearer (figure 7).

In addition to K117R, we also generated a version of pathogenic Atxn3 whose individual lysine residues were mutated into arginines, denoted as KNull. This transgene was generated to ask the questions: 1) is ubiquitination of pathogenic Atxn3 necessary for its degradation in vivo? We previously documented that wild-type Atxn3 does not need to be ubiquitinated to be degraded in cultured mammalian cells (HeLa, HEK-293) or in flies that expressed human, wild-type Atxn3 (Blount et al., 2020; Blount et al., 2014). Additionally, pathogenic Atxn3 does not need to be ubiquitinated to be degraded in cultured, HEK-293T mammalian cells (Blount et al., 2020). Still, the question remained whether ubiquitination is essential for the degradation of pathogenic Atxn3 in vivo. 2) We also wondered: does overall ubiquitination impact pathogenic Atxn3 toxicity?

The answer to the first question confirms our previous reports that ubiquitination is not an absolute requirement for the turnover of pathogenic Atxn3. This is not to say that there are not instances when ubiquitination regulates Atxn3 degradation; prior evidence towards this role is robust and instances when ubiquitination fine-tunes the degradation of this DUB are highly likely (Dantuma and Herzog, 2020; Johnson et al., 2022b; Lieberman et al., 2018; Matos et al., 2019b). The answer to the second question is not straightforward. According to biochemical examinations, KNull Atxn3(Q80) is more aggregation-prone than the version with all lysines present. However, the KNull version is also less toxic in each of the assays we tested in *Drosophila*. We propose that this reduced toxicity is due to the markedly lower levels of the KNull protein, similar to earlier work where we showed that two different isoforms of pathogenic Atxn3 have differing toxicities that are related to their abundance in fly cells: the more abundant isoform was more toxic than the less abundant one (Johnson et al., 2019). Overall, we conclude that lysine residues are important for both the aggregation and toxicity of pathogenic Atxn3.

K117 is not the only lysine residue modified on Atxn3 (Todi et al., 2010). A recent report from the Schmidt lab, which was published as we were completing this manuscript, indicated that lysine residues besides K117, especially those at positions 8 and 85, regulate the aggregation, localization and stability of this protein in cultured cells (Pereira Sena et al., 2023), underscoring the need for further investigations into the roles of these residues on Atxn3 and SCA3 pathogenesis.

There is prior evidence from the polyQ field that ubiquitination of a disease protein impacts its aggregation and toxicity, as reported for the Kennedy Disease protein, androgen receptor (Pluciennik et al., 2021; Sengupta et al., 2022). How might ubiquitination impact Atxn3 aggregation? Ubiquitinated, pathogenic Atxn3 may be less aggregation-prone due to steric hindrances that oppose oligomerization and aggregation of the disease protein. An additional, non-mutually exclusive mechanism may rely on ubiquitinated Atxn3 partnering up with other proteins through ubiquitin-binding sites, which can also hinder aggregation.

Various ubiquitin-related enzymes have been reported to ubiquitinate Atxn3, including the E2 conjugases Ubch5C and Ube2W, and the E3 ligases CHIP and Parkin (Dantuma and Herzog, 2020; Johnson et al., 2022b). In our prior work using *Drosophila* lines expressing wild-type Atxn3 (Tsou et al., 2013) and in additional experiments we conducted for this study with flies expressing pathogenic Atxn3 (Supplemental figure 2), we did not observe differences when Ubch5C or CHIP were knocked down individually in flies. We propose that Atxn3 is modified in vivo by more than one specific conjugase/ligase pair, and that individual targeting is insufficient to modify its ubiquitination pattern in this system.

The functions of Atxn3 remain to be elucidated. Studies conducted with reconstituted systems in vitro, in cultured mammalian cells, and in mouse models reveal a DUB that is involved in some aspects of protein quality control, including ER-Associated Degradation and autophagy (Liu and Ye, 2012; Zhong and Pittman, 2006); an enzyme that functions in sensing the overall levels of ubiquitin in the system (Dantuma and Herzog, 2020; Scaglione et al., 2011; Winborn et al., 2008); that regulates DNA-damage repair processes (Dantuma and Herzog, 2020; Matos et al., 2019a); and whose wild-type protein is involved in the visual system (Toulis et al., 2020). As a gene, *Atxn3* appears to be dispensable in mice (Reina et al., 2010; Schmitt et al., 2007; Switonski et al., 2011). The pathogenic polyQ expansion may perturb some of the functions of wild-type Atxn3, while also imparting news ones, resulting in neuronal and glial malfunction, clinical manifestation, and neurodegeneration. Ubiquitination of Atxn3 at K117 markedly enhances its activity as an enzyme in vitro and upregulates some of its cellular functions, such as aggresome formation and protections against proteotoxic stress (Burnett and Pittman, 2005; Todi et al., 2010; Tsou et al., 2013). Ubiquitination of pathogenic Atxn3 at K117 may enhance some of its normal functions, enhance some of its toxic, gain-of-function properties, or both. Based on our results that prohibiting ubiquitination at K117 increases the toxicity of pathogenic Atxn3 in flies, we suggest that ubiquitination of K117 on Atxn3 is largely protective in SCA3 (figure 7). The exact details require further investigations.

METHODS

Antibodies:

Anti-HA (rabbit monoclonal C29F4, 1:500-1000; Cell Signaling Technology)

Anti ataxin-3 (mouse monoclonal 1H9, MAB5360, 1:500-1000; Millipore)

Anti-lamin (mouse monoclonal ADL84.12-5, 1:1000; Developmental Studies Hybridoma Bank)

Anti-tubulin (mouse monoclonal T5168, 1:10,000; Sigma-Aldrich)

Anti-Flag (rabbit polyclonal SAB4301135, 1-1000; Sigma-Aldrich)

Drosophila lines:

UAS-Atxn3 transgenic lines were generated as described before (Johnson et al., 2019; Johnson et al., 2021; Johnson et al., 2022a; Ristic et al., 2018; Sutton et al., 2017). Full-length, human, pathogenic Atxn3 cDNA was synthesized de novo by Genscript (Genscript.com) with a CAGCAA doublet repeat to preclude mRNA toxicity and unconventional translation (Johnson et al., 2022a). K117R and KNull were generated by mutating the respective lysine codons of the pathogenic Atxn3 cDNA into arginine codons. The constructs were then sub-cloned into pWalium10.moe for PhiC31 integration into site attP2 of the third chromosome of the fly. FLAG-tagged UAS-DnaJ-1 was generated by synthesizing the cDNA of *Drosophila* DnaJ-1 de novo (Genscript), sub-cloning into pWalium10.moe, and using PhiC31 integration to insert into attp40 on the second chromosome of the fly. Transformants were examined by PCR for integration site and direction, and sequenced for construct integrity. sqh-Gal4 was a gift from Dr. Daniel Kiehart, Duke University. elav-Gal4 was a gift from Dr. Daniel Eberl, University of Iowa. elav-Gal4-GS was a gift from Dr. R. J. Wessells, Wayne State University. GMR-Gal4 was stock #8121 from Bloomington *Drosophila* Stock Center. Control flies consisted of a single outcross of the respective Gal4 driver into the same genetic background as each Atxn3 transgenic line, without expressing Atxn3.

Drosophila husbandry and longevity:

Flies were maintained at 25°C in diurnally-controlled incubators with 12 h light/dark cycles and on conventional cornmeal media. All offspring were maintained in the same conditions, with the exception of crosses that utilized elav-GS-Gal4. Those offspring were switched into media containing RU486 soon after emerging as adults to induce the expression of transgenes. In our hands, control flies maintained on media with RU486 or lacking RU486 behave similarly. For lifespan recordings, adult flies were collected each day and separated into groups of the same size (10 adults per vial) and gender. Flies were flipped into new food every other day. The total number of adults tracked (N) for each group is noted in figures. In case of developmental lethality, flies were observed from the embryo stage through eclosure or early adult death, and lethality was recorded multiple times per week. All flies were heterozygous for each constituent transgene.

Western blotting:

Western blotting was conducted using 5 adult flies (neuronal expression) or 5 dissected fly heads (eye expression) per sample. Samples were homogenized in boiling SDS lysis buffer (50 mM Tris pH 6.8, 2% SDS, 10% glycerol, 100 mM dithiothreitol (DTT)), sonicated, boiled for 10 min, and subsequently centrifuged for 10 min at 13,300 rpm at room temperature. Samples were electrophoresed through Tris/Glycine gels (Bio-Rad). Western blots were imaged using ChemiDoc (Bio-Rad). Quantification was conducted using ImageLab (Bio-Rad). We used direct blue stains of total protein as loading controls by saturating PVDF membrane for 10 min in 0.008% Direct Blue 71 (Sigma-Aldrich) dissolved in 40% ethanol and 10% acetic acid, rinsed with a solution of 40% ethanol/10% acetic acid, then ultra-pure water, and then air dried and imaged. For Western blotting of samples from cytoplasmic/nuclear separation, please see further below.

Co-immunopurifications:

Ten adult flies were thoroughly homogenized in 800 μL of buffer consisting of 1:1 NETN (50 mM Tris, pH 7.5, 150 mM NaCl, 0.5% Nonidet P-40)/PBS supplemented with protease inhibitors (PI; Sigma-Aldrich, S-8820). Homogenates were rotated at 4°C for 25 minutes and then centrifuged for 10 minutes at 5000 x g at 4°C. Supernatant was subsequently combined with bead-bound antibody and tumbled at 4°C for 4 hours. Beads were rinsed 5 times each with lysis buffer, and bead-bound complexes were eluted through Laemmli buffer (Bio-Rad) and heating at 95°C for 5 minutes. Supernatant was then supplemented with 6% SDS to a final concentration of 1.5% SDS and loaded for Western blotting.

qRT-PCR:

Relative message abundance from 6 individual samples per genotype was determined by amplification and staining with Power SYBR Green using the QuantStudio3 system and Design and Analysis 2.6.0 software (Applied Biosystems). *Rp49* abundance was used to calculate relative expression. Primer sequences are listed below:

rp49-F: 5’-AGATCGTGAAGAAGCGCACCAAG-3’,

rp49-R: 5’-CACCAGGAACTTCTTGAATCCGG-3’

ataxin-3-F: 5’-GAATGGCAGAAGGAGGAGTTACTA-3’

ataxin-3-R: 5’-GACCCGTCAAGAGAGAATTCAAGT-3’

DnaJ-1-F1: 5’-GTACAAGGAGGAGAAGGTGCTG-3’

DnaJ-1-R1: 5’-CAGACTGATCTGGGCTGTATACTT-3’

Nuclear/cytoplasmic fractionation:

Fractionation of nuclear and cytoplasmic fractions from *Drosophila* lysates was conducted with the ReadyPrep Protein Extraction Kit (Bio-Rad). Seven whole flies per group were homogenized in cytoplasmic extraction buffer (Bio-Rad) and subsequently processed as instructed by the manufacturer. Samples were then supplemented with SDS lysis buffer,

boiled for 10 minutes, electrophoresed on SDS-PAGE gels, and processed for Western blotting, as noted above.

Statistics:

Statistical analyses were conducted with GraphPad's Prism 9. Tests used are specified in the figure legends.

Supplementary Material

Refer to Web version on PubMed Central for supplementary material.

ACKNOWLEDGEMENTS:

We extend our gratitude to Era Cobani for her help with conducting several of the lifespan assays.

FUNDING:

This study was supported in part by NIGMS T34GM140932 (ALH) and NINDS R01NS086778 (SVT).

References

Bichelmeier U, et al. , 2007. Nuclear localization of ataxin-3 is required for the manifestation of symptoms in SCA3: In vivo evidence. Journal of Neuroscience. 27, 7418–7428. [PubMed: 17626202]

Blount JR, et al. , 2020. Degron capability of the hydrophobic C-terminus of the polyglutamine disease protein, ataxin-3. Journal of Neuroscience Research. 98, 2096–2108. [PubMed: 32643791]

Blount JR, et al. , 2018. Expression and Regulation of Deubiquitinase-Resistant, Unanchored Ubiquitin Chains in Drosophila. Sci Rep. 8, 8513. [PubMed: 29855490]

Blount JR, et al. , 2014. Ubiquitin-binding site 2 of ataxin-3 prevents its proteasomal degradation by interacting with Rad23. Nature Communications. 5.

Brand AH, et al. , 1994. Ectopic expression in Drosophila. Methods Cell Biol. 44, 635–54. [PubMed: 7707973]

Brand AH, Perrimon N, 1993. Targeted gene expression as a means of altering cell fates and generating dominant phenotypes. Development. 118, 401–15. [PubMed: 8223268]

Burnett BG, Pittman RN, 2005. The polyglutamine neurodegenerative protein ataxin 3 regulates aggresome formation. Proc Natl Acad Sci U S A. 102, 4330–5. [PubMed: 15767577]

Dantuma NP, Herzog LK, 2020. Machado-Joseph Disease: A Stress Combating Deubiquitylating Enzyme Changing Sides. Adv Exp Med Biol. 1233, 237–260. [PubMed: 32274760]

Faggiano S, et al. , 2013. Enzymatic production of mono-ubiquitinated proteins for structural studies: The example of the Josephin domain of ataxin-3. Febs Open Bio. 3, 453–458.

Faggiano S, et al. , 2015. Allosteric regulation of deubiquitylase activity through ubiquitination. Frontiers in Molecular Biosciences. 2.

Fish MP, et al. , 2007. Creating transgenic Drosophila by microinjecting the site-specific phiC31 integrase mRNA and a transgene-containing donor plasmid. Nat Protoc. 2, 2325–31. [PubMed: 17947973]

Groth AC, et al. , 2004. Construction of transgenic Drosophila by using the site-specific integrase from phage phiC31. Genetics. 166, 1775–82. [PubMed: 15126397]

Johnson SL, et al. , 2019. Differential toxicity of ataxin-3 isoforms in Drosophila models of Spinocerebellar Ataxia Type 3. Neurobiol Dis. 132, 104535. [PubMed: 31310802]

Johnson SL, et al. , 2021. Targeting the VCP-binding motif of ataxin-3 improves phenotypes in Drosophila models of Spinocerebellar Ataxia Type 3. Neurobiol Dis. 160, 105516. [PubMed: 34563642]

Johnson SL, et al. , 2022a. Drosophila as a Model of Unconventional Translation in Spinocerebellar Ataxia Type 3. Cells. 11.

Johnson SL, et al. , 2020. Ubiquitin-interacting motifs of ataxin-3 regulate its polyglutamine toxicity through Hsc70-4-dependent aggregation. Elife. 9.

Johnson SL, et al. , 2022b. A survey of protein interactions and posttranslational modifications that influence the polyglutamine diseases. Front Mol Neurosci. 15, 974167. [PubMed: 36187346]

Joshi BS, et al. , 2021. DNAJB6b-enriched small extracellular vesicles decrease polyglutamine aggregation in in vitro and in vivo models of Huntington disease. iScience. 24, 103282. [PubMed: 34755099]

Kakkar V, et al. , 2012. DNAJ proteins and protein aggregation diseases. Curr Top Med Chem. 12, 2479–90. [PubMed: 23339302]

Kawaguchi Y, et al. , 1994. CAG expansions in a novel gene for Machado-Joseph disease at chromosome 14q32.1. Nat Genet. 8, 221–8. [PubMed: 7874163]

Kazemi-Esfarjani P, Benzer S, 2000. Genetic suppression of polyglutamine toxicity in Drosophila. Science. 287, 1837–40. [PubMed: 10710314]

Kuhlbrodt K, et al. , 2011. The Machado-Joseph disease deubiquitylase ATX-3 couples longevity and proteostasis. Nat Cell Biol. 13, 273–81. [PubMed: 21317884]

Lieberman AP, et al. , 2018. Polyglutamine Repeats in Neurodegenerative Diseases. Annu Rev Pathol.

Liu YF, Ye YH, 2012. Roles of p97-Associated Deubiquitinases in Protein Quality Control at the Endoplasmic Reticulum. Current Protein & Peptide Science. 13, 436–446. [PubMed: 22812527]

Markstein M, et al. , 2008. Exploiting position effects and the gypsy retrovirus insulator to engineer precisely expressed transgenes. Nat Genet. 40, 476–83. [PubMed: 18311141]

Matos CA, et al. , 2019a. Machado-Joseph disease/spinocerebellar ataxia type 3: lessons from disease pathogenesis and clues into therapy. Journal of Neurochemistry. 148, 8–28. [PubMed: 29959858]

Matos CA, et al. , 2019b. Machado-Joseph disease/spinocerebellar ataxia type 3: lessons from disease pathogenesis and clues into therapy. J Neurochem. 148, 8–28. [PubMed: 29959858]

Ni JQ, et al. , 2008. Vector and parameters for targeted transgenic RNA interference in Drosophila melanogaster. Nat Methods. 5, 49–51. [PubMed: 18084299]

Paulson HL, et al. , 2017. Polyglutamine spinocerebellar ataxias - from genes to potential treatments. Nat Rev Neurosci. 18, 613–626. [PubMed: 28855740]

Pereira Sena P, et al. , 2023. Implications of specific lysine residues within ataxin-3 for the molecular pathogenesis of Machado-Joseph disease. Front Mol Neurosci. 16, 1133271. [PubMed: 37273907]

Pluciennik A, et al. , 2021. Deubiquitinase USP7 contributes to the pathogenicity of spinal and bulbar muscular atrophy. J Clin Invest. 131.

Prifti MV, et al. , 2022. Ubiquitin-binding site 1 of pathogenic ataxin-3 regulates its toxicity in Drosophila models of Spinocerebellar Ataxia Type 3. Front Neurosci. 16, 1112688. [PubMed: 36733922]

Reina CP, et al. , 2010. Proteotoxic stress increases nuclear localization of ataxin-3. Hum Mol Genet. 19, 235–49. [PubMed: 19843543]

Ristic G, et al. , 2018. Toxicity and aggregation of the polyglutamine disease protein, ataxin-3 is regulated by its binding to VCP/p97 in Drosophila melanogaster. Neurobiology of Disease. 116, 78–92. [PubMed: 29704548]

Roman G, Davis RL, 2002. Conditional expression of UAS-transgenes in the adult eye with a new gene-switch vector system. Genesis. 34, 127–31. [PubMed: 12324966]

Scaglione KM, et al. , 2011. Ube2w and ataxin-3 coordinately regulate the ubiquitin ligase CHIP. Mol Cell. 43, 599–612. [PubMed: 21855799]

Schmidt T, et al. , 1998. An isoform of ataxin-3 accumulates in the nucleus of neuronal cells in affected brain regions of SCA3 patients. Brain Pathology. 8, 669–679. [PubMed: 9804376]

Schmitt I, et al. , 2007. Inactivation of the mouse Atxn3 (ataxin-3) gene increases protein ubiquitination. Biochem Biophys Res Commun. 362, 734–9. [PubMed: 17764659]

Sengupta M, et al. , 2022. The role of ubiquitination in spinal and bulbar muscular atrophy. Front Mol Neurosci. 15, 1020143. [PubMed: 36277484]

Stevanin G, et al. , 1995a. Linkage disequilibrium at the Machado-Joseph disease/spinal cerebellar ataxia 3 locus: evidence for a common founder effect in French and Portuguese-Brazilian families as well as a second ancestral Portuguese-Azorean mutation. Am J Hum Genet. 57, 1247–50. [PubMed: 7485178]

Stevanin G, et al. , 1995b. The gene for spinal cerebellar ataxia 3 (SCA3) is located in a region of approximately 3 cM on chromosome 14q24.3-q32.2. Am J Hum Genet. 56, 193–201. [PubMed: 7825578]

Sutton JR, et al. , 2017. Interaction of the polyglutamine protein ataxin-3 with Rad23 regulates toxicity in Drosophila models of Spinocerebellar Ataxia Type 3. Hum Mol Genet. 26, 1419–1431. [PubMed: 28158474]

Switonski PM, et al. , 2011. Mouse ataxin-3 functional knock-out model. Neuromolecular Med. 13, 54–65. [PubMed: 20945165]

Todi SV, et al. , 2007. Cellular turnover of the polyglutamine disease protein ataxin-3 is regulated by its catalytic activity. J Biol Chem. 282, 29348–58. [PubMed: 17693639]

Todi SV, et al. , 2010. Activity and Cellular Functions of the Deubiquitinating Enzyme and Polyglutamine Disease Protein Ataxin-3 Are Regulated by Ubiquitination at Lysine 117. Journal of Biological Chemistry. 285, 39303–39313. [PubMed: 20943656]

Todi SV, et al. , 2009. Ubiquitination directly enhances activity of the deubiquitinating enzyme ataxin-3. EMBO J. 28, 372–82. [PubMed: 19153604]

Toulis V, et al. , 2020. The Deubiquitinating Enzyme Ataxin-3 Regulates Ciliogenesis and Phagocytosis in the Retina. Cell Rep. 33, 108360. [PubMed: 33176149]

Tsou WL, et al. , 2013. Ubiquitination regulates the neuroprotective function of the deubiquitinase ataxin-3 in vivo. J Biol Chem. 288, 34460–9. [PubMed: 24106274]

Tsou WL, et al. , 2015a. DnaJ-1 and karyopherin alpha3 suppress degeneration in a new Drosophila model of Spinocerebellar Ataxia Type 6. Hum Mol Genet. 24, 4385–96. [PubMed: 25954029]

Tsou WL, et al. , 2015b. The deubiquitinase ataxin-3 requires Rad23 and DnaJ-1 for its neuroprotective role in Drosophila melanogaster. Neurobiol Dis. 82, 12–21. [PubMed: 26007638]

Winborn BJ, et al. , 2008. The deubiquitinating enzyme ataxin-3, a polyglutamine disease protein, edits Lys63 linkages in mixed linkage ubiquitin chains. J Biol Chem. 283, 26436–43. [PubMed: 18599482]

Zhong X, Pittman RN, 2006. Ataxin-3 binds VCP/p97 and regulates retrotranslocation of ERAD substrates. Hum Mol Genet. 15, 2409–20. [PubMed: 16822850]

Zoghbi HY, Orr HT, 2009. Pathogenic mechanisms of a polyglutamine-mediated neurodegenerative disease, spinocerebellar ataxia type 1. J Biol Chem. 284, 7425–9. [PubMed: 18957430]

Highlights

- Mutations in the deubiquitinase Ataxin-3 cause Spinocerebellar Ataxia Type 3
- Ataxin-3 is modified post-translationally by ubiquitin on lysine residues
- We examined the effect of ubiquitination on pathogenic Ataxin-3 by mutating lysines
- We found that ubiquitination mildly impacts Ataxin-3 toxicity in fly disease models

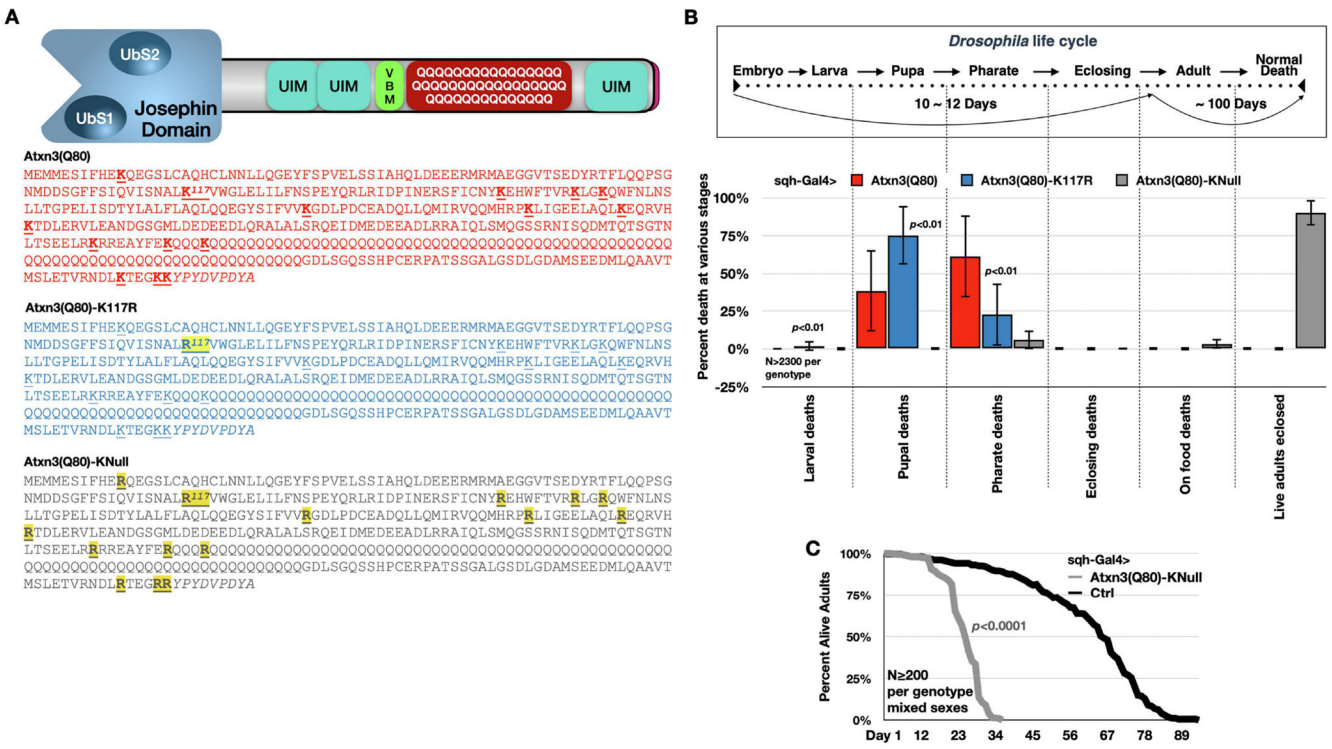

Figure 1: K117 mutation enhances Atxn3 toxicity in all tissues

A) Atxn3 protein domains and the sequences encoded by the transgenes in this study. UbS: ubiquitin-binding site. UIM: ubiquitin-binding motif. VBM: VCP-binding motif. HA tag is appended inline to each protein (sequence in italics). Josephin domain is the catalytic portion of Atxn3.

B) Results of sqh-Gal4 (ubiquitous driver) expressing the indicated Atxn3 forms. All genotypes were heterozygous sqh-Gal4 in trans with the indicated UAS-Atxn3 transgene, also heterozygous. Means −/+ SD. Statistics: t-tests comparing Atxn3(Q80)-K117R to Atxn3(Q80).

C) Longevity of adult flies that eclosed successfully from (B). Ctrl: sqh-Gal4 in trans with the parental line used to generate the Atxn3 transgenics. Statistics: log-rank test.

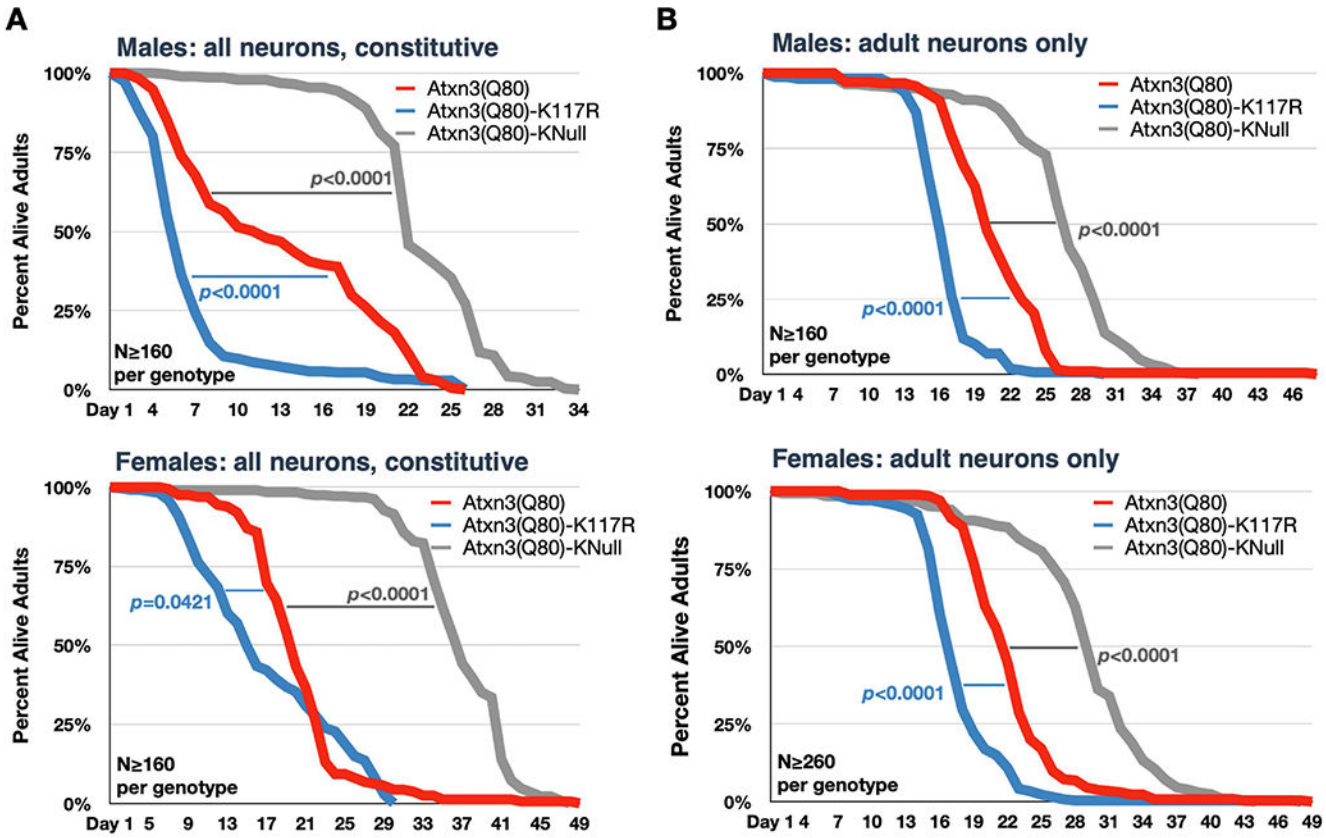

Figure 2: K117 mutation enhances Atxn3 toxicity in neurons

A, B) Longevity of adult flies expressing the noted versions of Atxn3 in all neuronal cells. Heterozygous driver (elav-Gal4, panel A; elav-GS-Gal4, panel B) was in trans with the noted Atxn3 transgenes, also heterozygous. Statistics: log-rank tests. For adult-only expression, we utilized the GeneSwitch Gal4-UAS system, which needs the presence of the inducer, RU486 to express a specific UAS transgene. We reared flies in media without RU486 until the day that they eclosed from their pupal cases, and then moved them onto media containing RU486, enabling the expression of human Atxn3 transgenes. These flies were maintained in media with RU486 until they all died.

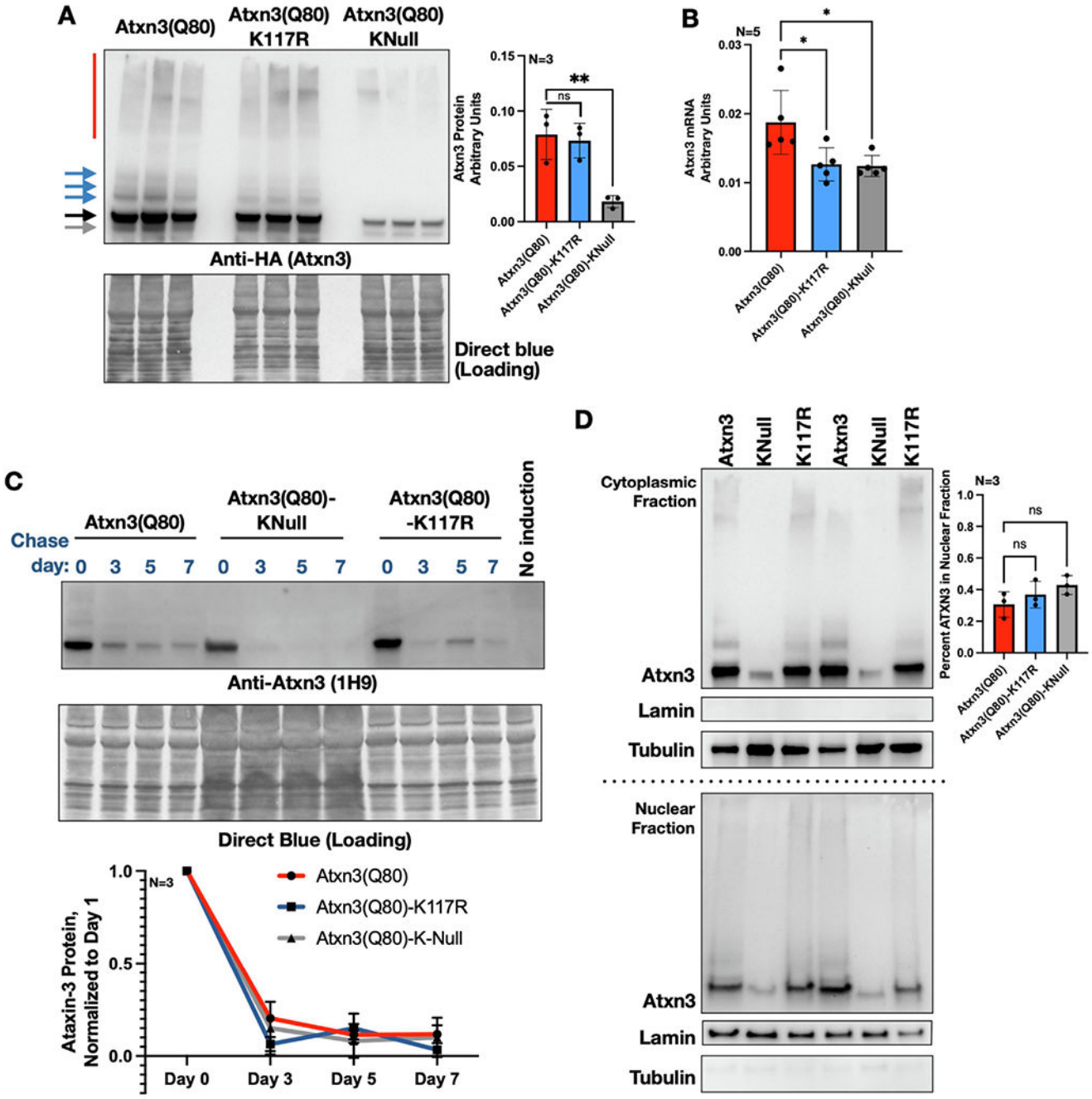

Figure 3: Effects of lysine mutations on the turnover and subcellular fractionation of pathogenic Atxn3

A) Western blots from adult female flies expressing the noted versions of Atxn3 constitutively in all neurons. Flies were heterozygous for driver (elav-Gal4) and Atxn3. Day 1 adults. Each lane represents an independent repeat. Black arrow: main, unmodified Atxn3. Blue arrow: ubiquitinated Atxn3, based on our previously published work (Blount et al., 2020; Johnson et al., 2019; Sutton et al., 2017; Todi et al., 2007; Todi et al., 2010; Todi et al., 2009; Tsou et al., 2013). Gray arrow: likely proteolytic fragment we observe sometimes. Red bar: SDS-resistant Atxn3. Quantifications: images from the left were used

for quantification, normalized to their respective Direct blue loading control. The entire Atxn3 signal was utilized, main band to top, including SDS-soluble and SDS-resistant species. Means −/+ SD. Statistics: one-way ANOVA with Dunnett's post hoc. **: $p<0.001$.

B) qRT-PCR results from 1-day-old adult females constitutively expressing the noted Atxn3 versions in all neurons, as in panel A. Means −/+ SD. Statistics: one-way ANOVA with Dunnett's post hoc. *: $p<0.05$.

C) Top: Western blots from adult female flies expressing the noted versions of Atxn3 in neurons for 7 days (+RU486) then allowed to degrade Atxn3 over the indicated timeline (−RU486). A higher amount of lysates from KNull was loaded to equilibrate as much as possible starting amounts at day 0. Bottom: quantification of signal from the top and additional independent repeats, normalized to respective day 0 levels. No statistical significances found were with oneway ANOVA with Dunnett's post hoc among day 3, 5 and 7 comparisons. This experiment was repeated independently 3 times, with 5 whole flies used per group per Western blot in each repeat. Flies were heterozygous for driver (elav-GS-Gal4) and Atxn3.

D) Left: Western blots of nuclear/cytoplasmic fractionations of Atxn3 versions noted expressed constitutively in all neurons. Flies were 1-day-old females. Right: quantification of images from the left and other independent repeats. Means −/+ SD. Statistics: one-way ANOVA with Dunnett's post hoc. Flies were heterozygous for driver (elav-Gal4) and Atxn3 transgenes. ns: not significant.

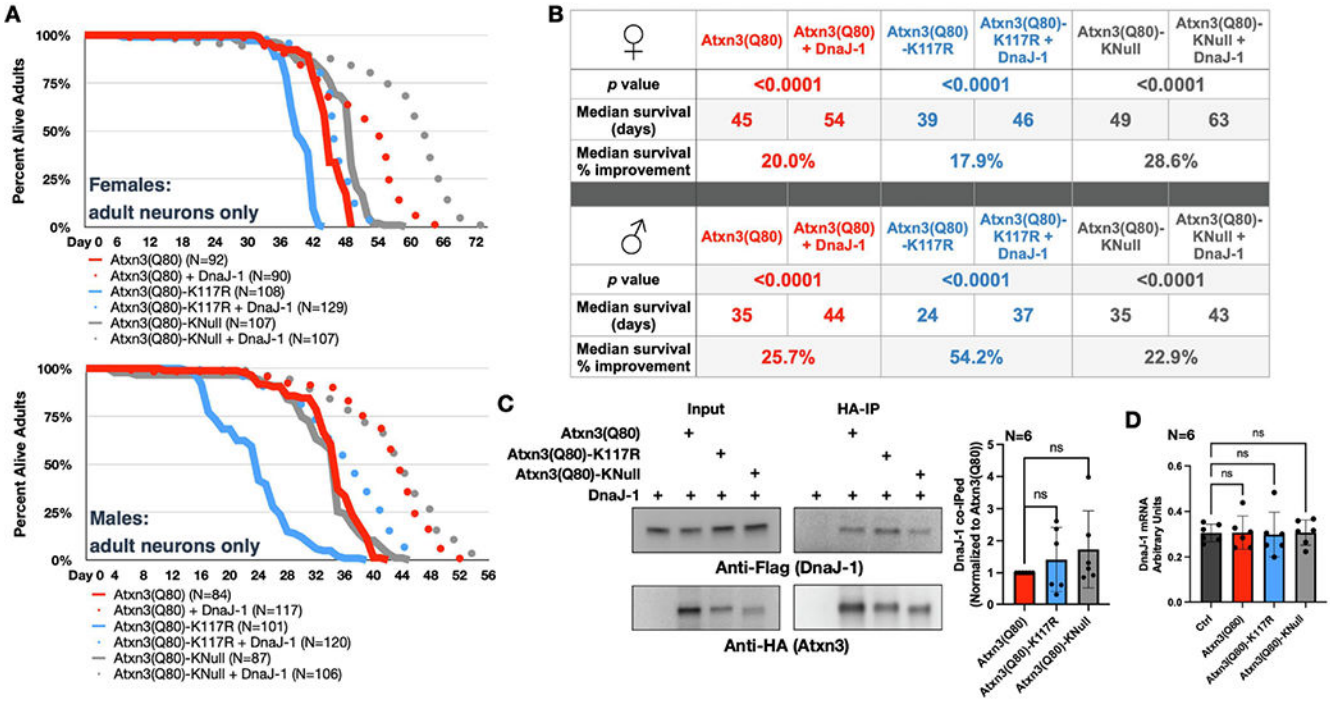

♀

	Atxn3(Q80)	Atxn3(Q80) + DnaJ-1	Atxn3(Q80) -K117R	Atxn3(Q80)- K117R + DnaJ-1	Atxn3(Q80)- KNull	Atxn3(Q80)- KNull + DnaJ-1
p value	<0.0001		<0.0001		<0.0001	
Median survival (days)	45	54	39	46	49	63
Median survival % improvement	20.0%		17.9%		28.6%	

♂

	Atxn3(Q80)	Atxn3(Q80) + DnaJ-1	Atxn3(Q80) -K117R	Atxn3(Q80)- K117R + DnaJ-1	Atxn3(Q80)- KNull	Atxn3(Q80)- KNull + DnaJ-1
p value	<0.0001		<0.0001		<0.0001	
Median survival (days)	35	44	24	37	35	43
Median survival % improvement	25.7%		54.2%		22.9%	

Figure 4: DnaJ-1 suppresses toxicity of pathogenic Atxn3 independently of lysine mutations

A, B) Longevity outcomes from adult flies expressing the noted versions of Atxn3 in the presence or absence of exogenous DnaJ-1, only in adult neurons. B) Statistics: log-rank tests.

C) Left: Western blots from co-immunopurifications of Atxn3 expressed in female adult neurons for 7 days in the presence of exogenous FLAG-tagged DnaJ-1. Right: quantifications from the left and other independent repeats. Statistics: Wilcoxon tests. ns: not significant. FLAG-tagged DnaJ-1 was used for these studies since antibodies to detect endogenous DnaJ-1 are not available. Flies were heterozygous for the Gal4 driver and each UAS transgenes.

D) qRT-PCR of endogenous levels of DnaJ-1 when Atxn3 of the noted versions was expressed. Statistics: one-way ANOVA with Dunnett's post-hoc. ns: not significant.

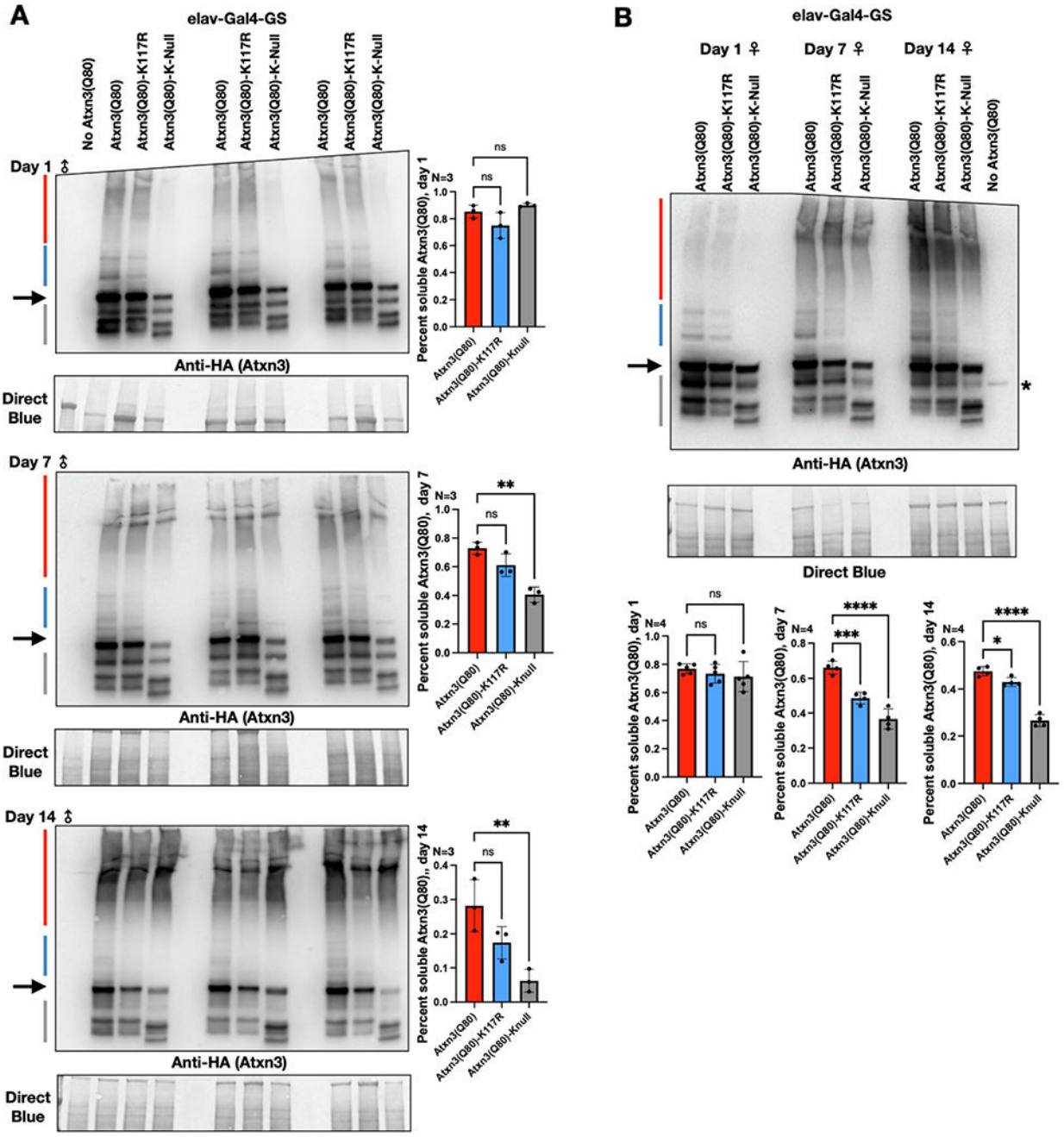

Figure 5: Lysine mutations increase levels of SDS-resistant species of pathogenic Atxn3 in adult neurons

A, B) Western blots from flies expressing the noted versions of Atxn3 in adult neurons for the indicated amounts of time. Black arrow: main, unmodified Atxn3. Blue bar: ubiquitinated Atxn3. Red bar: SDS-resistant Atxn3. Gray bar: proteolytic fragments of Atxn3. Asterisk on the right of blot in 5B is non-specific signal. Associated quantifications are from these blots. Means −/+ SD. Atxn3 signal for each lane was calculated by quantifying separately the SDS-soluble species (main band + ubiquitinated species) and the SDS-resistant species, then expressing soluble Atxn3 as percent fraction of the total Atxn3

signal in that lane, using the formula: 100% X SDS-soluble / (SDS-soluble + SDS-resistant). Statistics: one-way ANOVA with Dunnett's post hoc. ns: not significant. *: $p<0.05$. ***: $p<0.001$. ****: $p<0.0001$. Flies were heterozygous for driver and Atxn3.

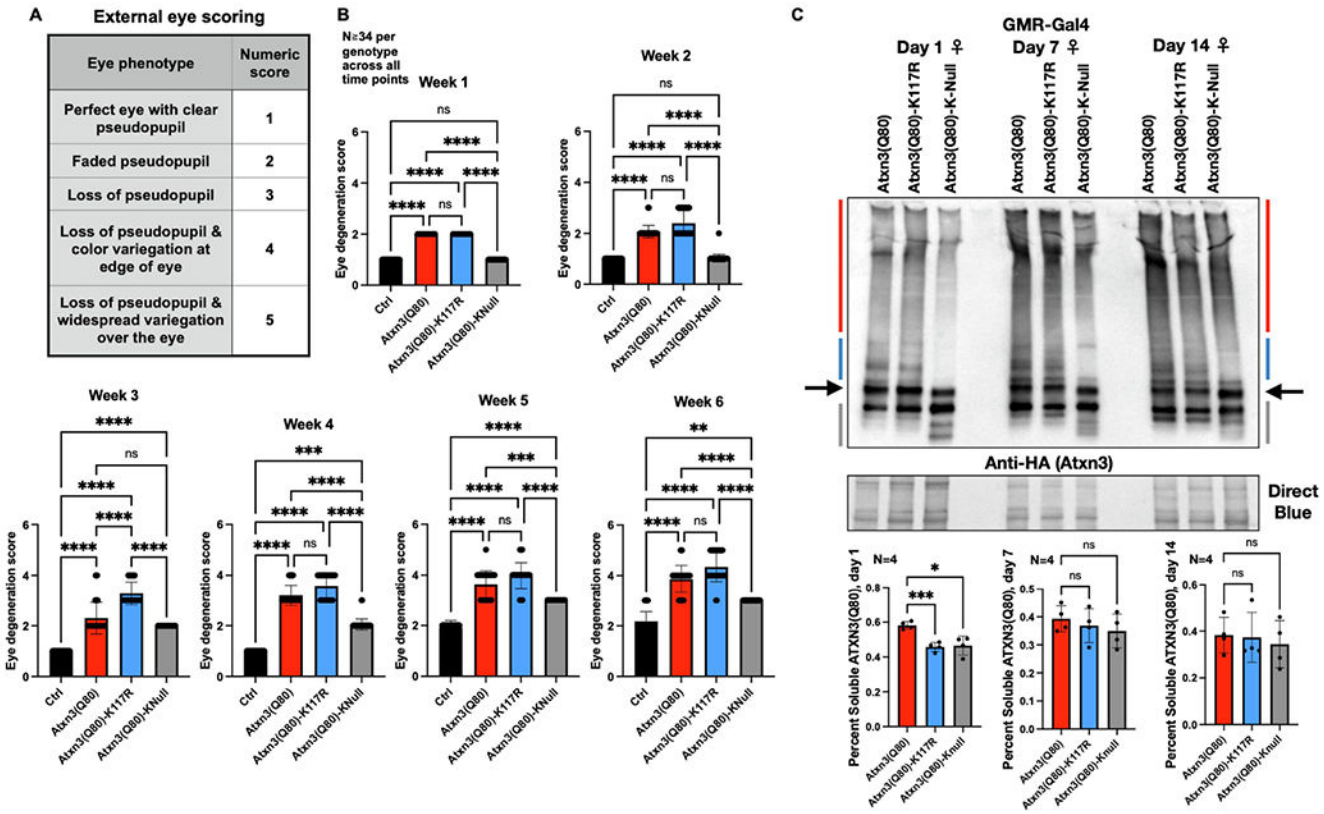

Figure 6: Lysine mutations impact the toxicity of pathogenic Atxn3 in fly eyes

A) Eye scoring system.

B) Means −/+ SD of eye phenotypes when the noted versions of Atxn3 are expressed in fly eyes (GMR-Gal4). ns: not significant. **: p<0.01. ***: p<0.001. ****: p<0.0001.

C) Western blots and related quantifications from 1-day-old adult female fly heads. GMR-Gal4 was the driver in each case. Black arow: main ATxn3. Blue bar: ubiquitinated Atxn3. Red bar: SDS-resistant Atxn3. Gray bar: proteolytic fragments of Atxn3. Proteolytic species differ depending on the tissues in which Atxn3 is expressed in flies and also vary among blots and antibodies (Blount et al., 2020; Blount et al., 2014; Johnson et al., 2019; Johnson et al., 2021; Johnson et al., 2022a; Sutton et al., 2017; Todi et al., 2010). Quantifications are from the top and additional independent repeats. Atxn 3 signal for each lane was calculated by quantifying SDS-soluble species, SDS-resistant species, and expressed as percent soluble fraction of the total Atxn3 signal in that lane. Means −/+ SDS. Statistics: Brown-Forsythe and Welch ANOVA tests. ns: not significant; *: p<0.05. ***: p<0.001. All flies were heterozygous for driver and Atxn3 transgenes.

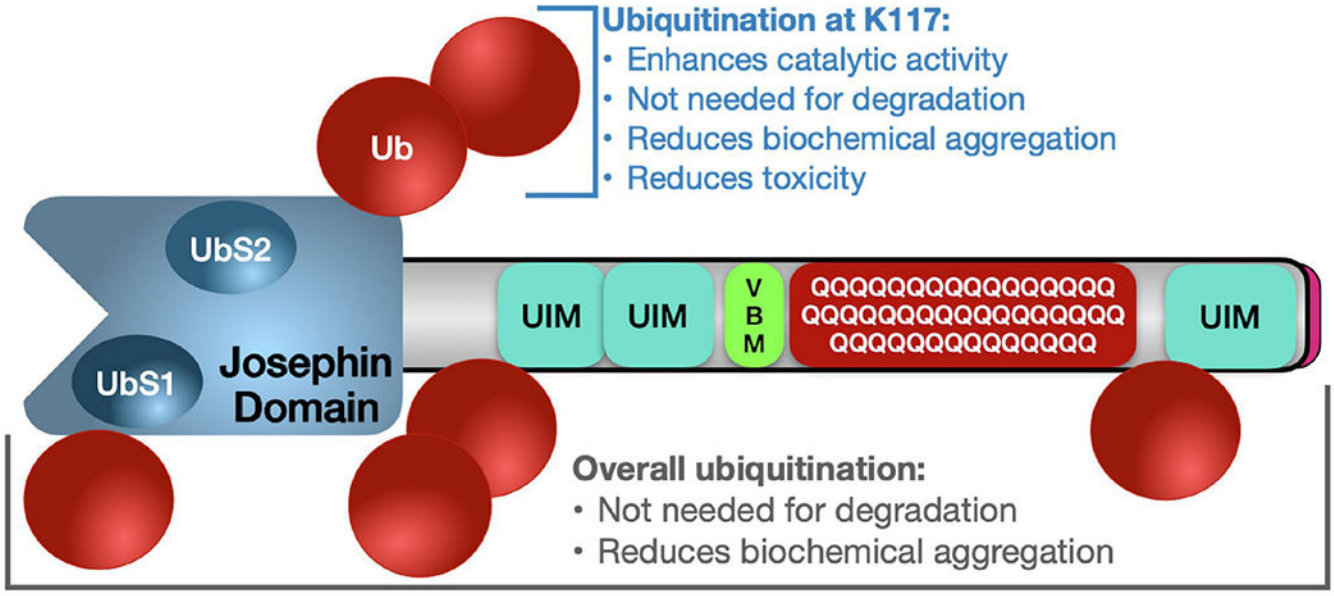

Figure 7: Summary

Brief summary of the findings supported from our current data and prior publications in the discussion section.